

## Supplemental Materials

### **Co-SrCO<sub>3</sub>/N-doped carbon: a highly efficient hybrid electrocatalyst for oxygen reduction reaction and Zn-air battery**

Xiaobo He <sup>b, c</sup>, Fengxiang Yin <sup>a, b, c \*</sup>, Jinnan Chen <sup>a</sup> and Caiyun Ye <sup>a</sup>

<sup>a</sup> State Key Laboratory of Organic-inorganic Composites, Beijing University of Chemical Technology, Beijing 100029, PR China

<sup>b</sup> Advanced Catalysis and Green Manufacturing Collaborative Innovation Center, Changzhou University, Changzhou 213164, Jiangsu, PR China

<sup>c</sup> Changzhou Institute of Advanced Materials, Beijing University of Chemical Technology, Changzhou 213164, PR China

\* Corresponding author.

Tel.: +86 10 64412054; fax: +86 10 64419619.

E-mail address: yinfx@mail.buct.edu.cn (F. Yin).

## Supplemental Tables

**Table S1** Binding energy of different species determined by XPS.

Samples	Co 2p <sub>3/2</sub> (eV)			Sr 3d <sub>5/2</sub> (eV)		N 1s (eV)		
	Co <sup>0</sup>	Co <sup>2+</sup>	Co <sup>3+</sup>	SrO	SrCO <sub>3</sub>	Pyridinic N	Pyrrolic N	Quaternary N
Co-SrCO <sub>3</sub> /NC-500	777.6	780.6	779.3	133.3	134.2	398.5	400.1	401.3
Co-SrCO <sub>3</sub> /NC-600	778.6	781.7	780.1	133.4	134.1	398.0	399.5	400.6
Co-SrCO <sub>3</sub> /NC-700	778.3	780.9	779.5	133.2	134.0	398.2	400.0	401.1
SrCO <sub>3</sub> /NC-600	-	-	-	133.3	133.9	398.8	400.3	401.5
Co/NC-600	777.9	781.3	779.6	-	-	398.4	399.9	400.9

**Table S2** Surface composition of the prepared electrocatalysts and the reference samples determined by XPS

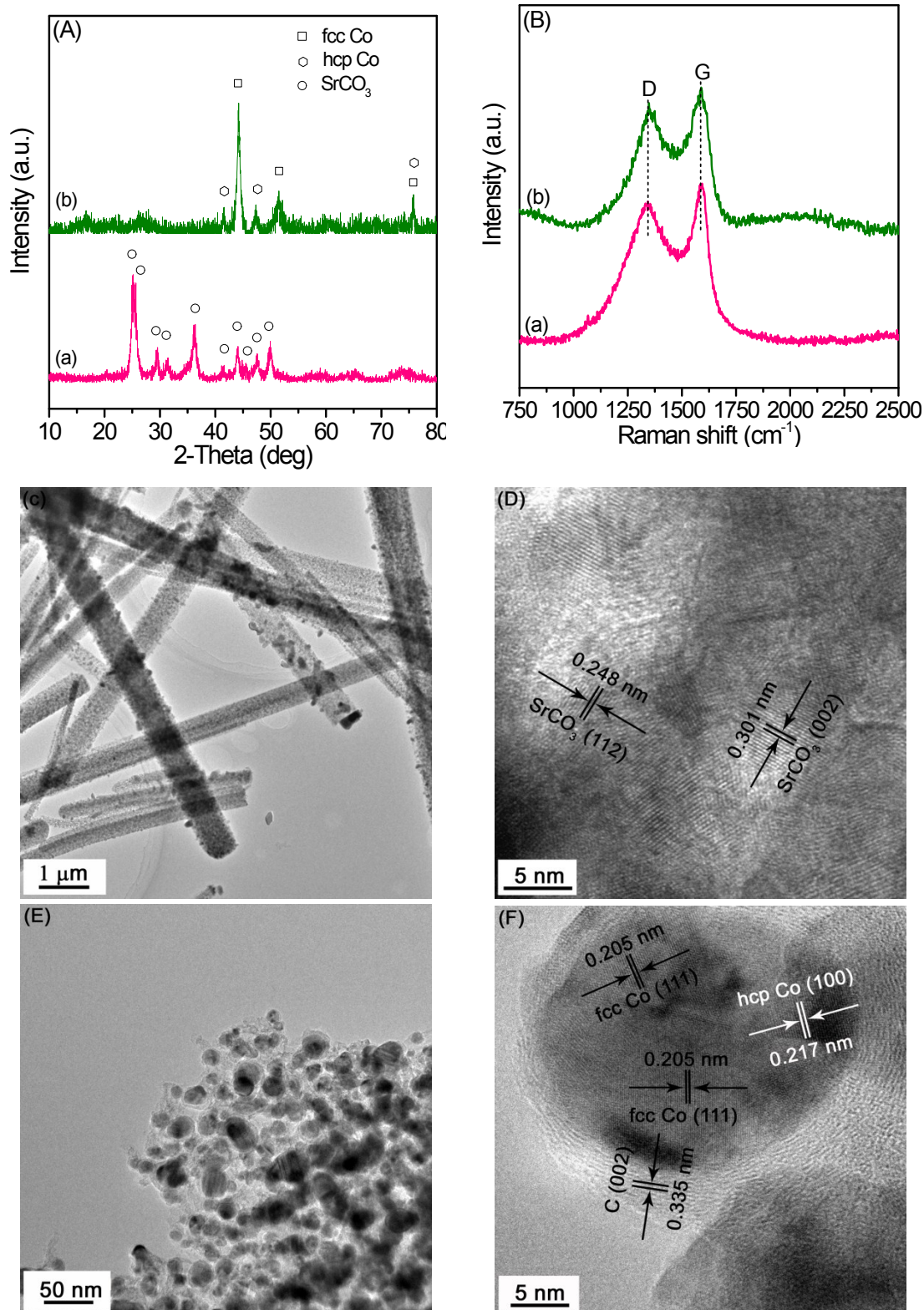
Samples	C (at.%)	O (at.%)	N (at.%)	Co (at.%)	Sr (at.%)	$\text{Sr}_{\text{oxide}}/\text{Sr}_{\text{carbonate}}$	SrO (at.%)
Co-SrCO <sub>3</sub> /NC-500	69.78	12.75	12.13	3.03	2.31	0.75	0.99
Co-SrCO <sub>3</sub> /NC-600	76.25	11.87	6.56	2.99	2.33	1.52	1.41
Co-SrCO <sub>3</sub> /NC-700	79.62	12.82	2.20	3.01	2.35	1.16	1.26
SrCO <sub>3</sub> /NC-600	71.21	18.77	1.60	--	8.42	0.83	3.82
Co/NC-600	84.85	5.65	6.60	2.90	--	--	--

**Table S3** The ORR activity of the reference samples.

Samples	Onset potential (V vs. RHE)	Half-wave potential ( $E_{1/2}$ , V vs. RHE)	Potential @ -3 mA cm <sup>-2</sup> ( $E_{j=-3}$ , V vs. RHE)	Limiting current density (mA cm <sup>-2</sup> )	Mass activity (A g <sup>-1</sup> ) <sup>a</sup>	Tafel slope (mV dec <sup>-1</sup> )	%HO <sub>2</sub> <sup>-</sup> (%)	n (electron transfer number)
SrCO <sub>3</sub> /NC-600	0.81	0.70	0.66	4.02	0.70	75.5	18.7	3.64
Co/NC-600	0.88	0.76	0.71	4.21	10.46	77.1	15.3	3.78

<sup>a</sup> The mass activity of the reference samples was determined through normalization of kinetic current density at 0.8 V (vs. RHE) to the corresponding mass loading (~0.12 mg cm<sup>-2</sup>).

## Supplemental Figures



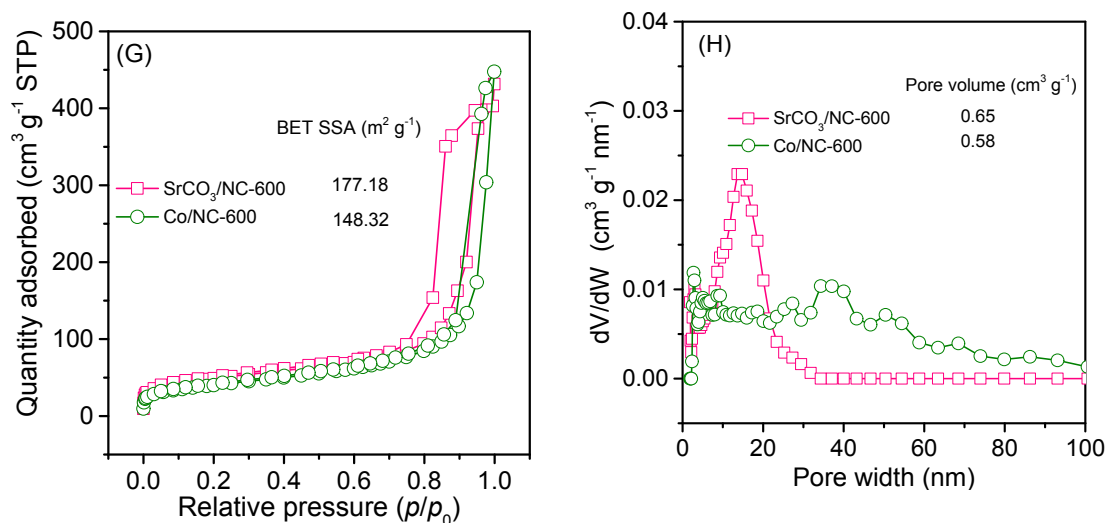


**Fig. S1.** XRD patterns (A) and Raman spectra (B) of SrCO<sub>3</sub>/NC-600 (a) and Co/NC-600 (b). TEM (C) and HRTEM (D) images of SrCO<sub>3</sub>/NC-600; TEM (E) and HRTEM (F) images of Co/NC-600. N<sub>2</sub> adsorption-desorption isotherms (G) and the corresponding pore size distributions (H) of SrCO<sub>3</sub>/NC-600 and Co/NC-600.

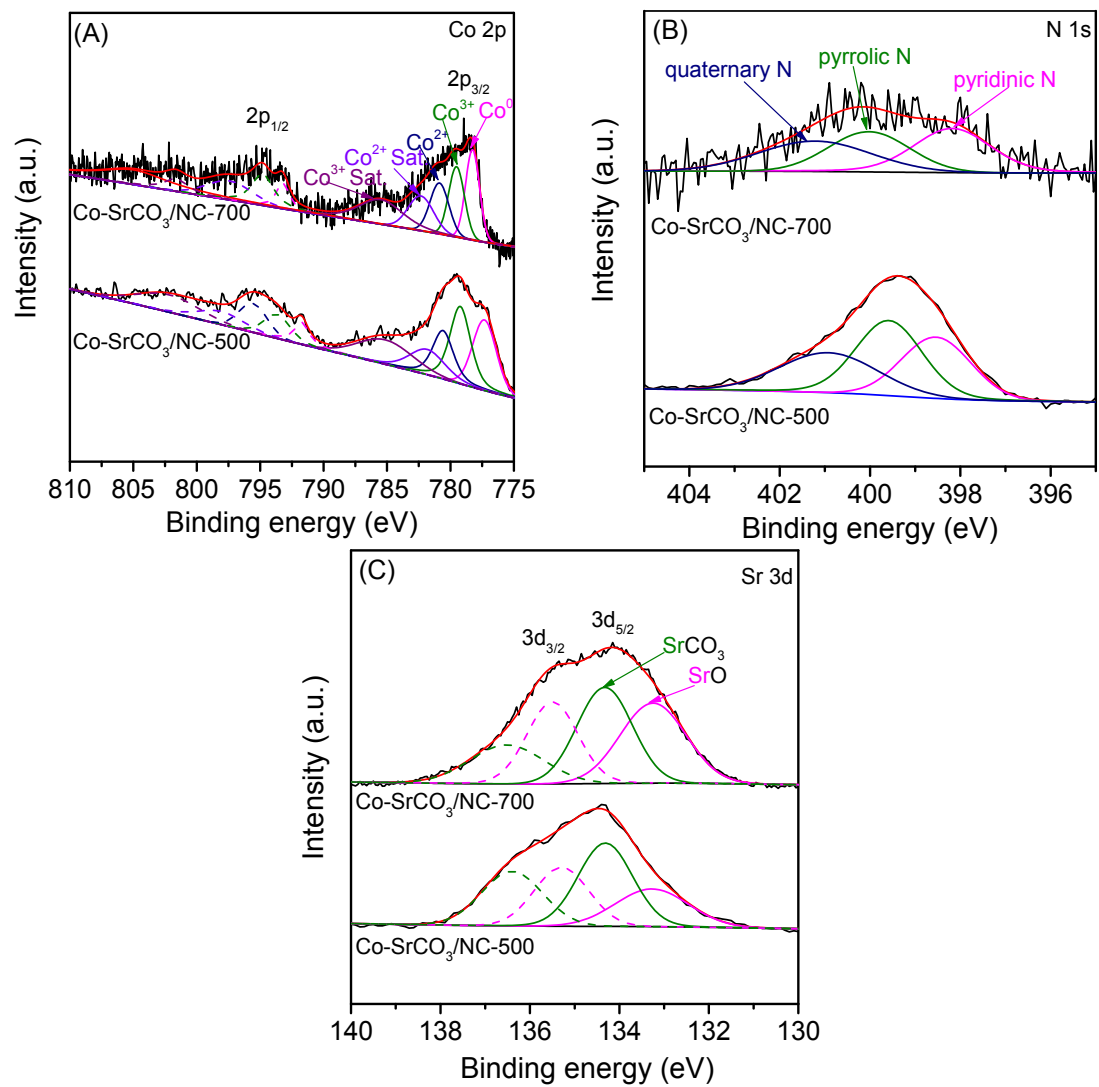


**Fig. S2.** XPS spectra of Co 2p (A), N 1s (B) and Sr 3d (C) for Co-SrCO<sub>3</sub>/NC-500 and -700.

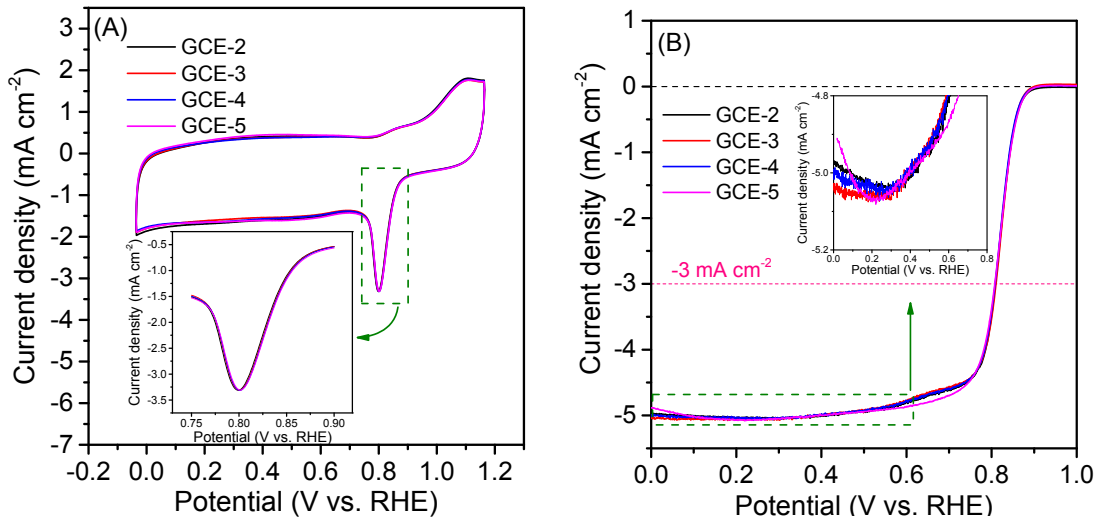


**Fig. S3** (A) CVs curves in O<sub>2</sub>-saturated 0.1 M KOH at 50 mV s<sup>-1</sup> and (B) ORR LSV curves at 1600 rpm and at 5 mV s<sup>-1</sup> for GCE-2, 3, 4 and 5.

**Notes:** To evaluate the effects of Nafion, we have used Co-SrCO<sub>3</sub>/NC-600 as the typical electrocatalyst to prepare several glassy carbon electrodes (GCEs), including the ones with both Nafion and electrocatalysts (GCE-1, 2, 3, 4 and 5) and the one with only Co-SrCO<sub>3</sub>/NC-600 but without Nafion (GCE-6). The preparation of the inks for GCE-1, 2, 3, 4 and 5 is similar to that described in the experimental section of manuscript. Briefly, 2.5 mg of Co-SrCO<sub>3</sub>/NC-600 and X μL of Nafion (5 wt%, Alfa Aesar) were dispersed in 1 mL anhydrous ethanol, where X is 10, 20, 40, 100 and 120. A homogeneous ink was obtained after ultra-sonication for 30 min. Before preparing the working electrode, the glassy carbon (GC) disk of GCE was polished to a mirror finish. Then, ~Y μL of the ink was casted onto the GC disk (~0.247 cm<sup>2</sup>), where Y is ~11.9, 12.1, 12.3, 13.0 and 13.3 for GCE-1, 2, 3, 4 and 5, respectively. GCE-1, 2, 3, 4 and 5 have the different feeding volume of Nafion per milligram of feeding Co-SrCO<sub>3</sub>/NC-600, i.e., 4, 8, 16, 40 and 48 μL mg<sub>cat</sub><sup>-1</sup> for GCE-1, 2, 3, 4 and 5, respectively, while keeping the same mass loading of ~0.12 mg cm<sup>-2</sup> for Co-SrCO<sub>3</sub>/NC-600.

$\text{SrCO}_3/\text{NC}-600$ . It should be noted that  $\text{Co-SrCO}_3/\text{NC}-600$  was unable to adhere to the surface of GCE-1 with little amount of Nafion and GCE-6 without Nafion.  $\text{Co-SrCO}_3/\text{NC}-600$  was prone to detach from GCE-1 and -6 easily during the measurement of ORR activity. On the contrary, for the other GCEs,  $\text{Co-SrCO}_3/\text{NC}-600$  can be attached to their surfaces firmly with the more Nafion. It indicates that Nafion as a polymer binder plays an important role in forming a stable film of electrocatalysts on the surface of GCEs, when an appropriate amount of Nafion is casted onto the surface of GCEs. As a result, the evaluation of the ORR activity for GCE-1 and -6 failed. The CVs curves in  $\text{O}_2$ -saturated 0.1 M KOH and the ORR LSV curves for GCE-2, 3, 4, and 5 are shown in Fig. S3A and S3B, respectively. Although the CV curves of the GCE-2~5 seem to be similar, they still show the differences from each other. The cathode peak marked by the green dotted pane are slight different, as indicated in the inset of Fig. S3A. The similar things happen to their LSV curves (Fig. S3B). As shown in the enlarged views (the inset of Fig. S3B), the mass-transport processes of these GCEs are slightly different from each other.

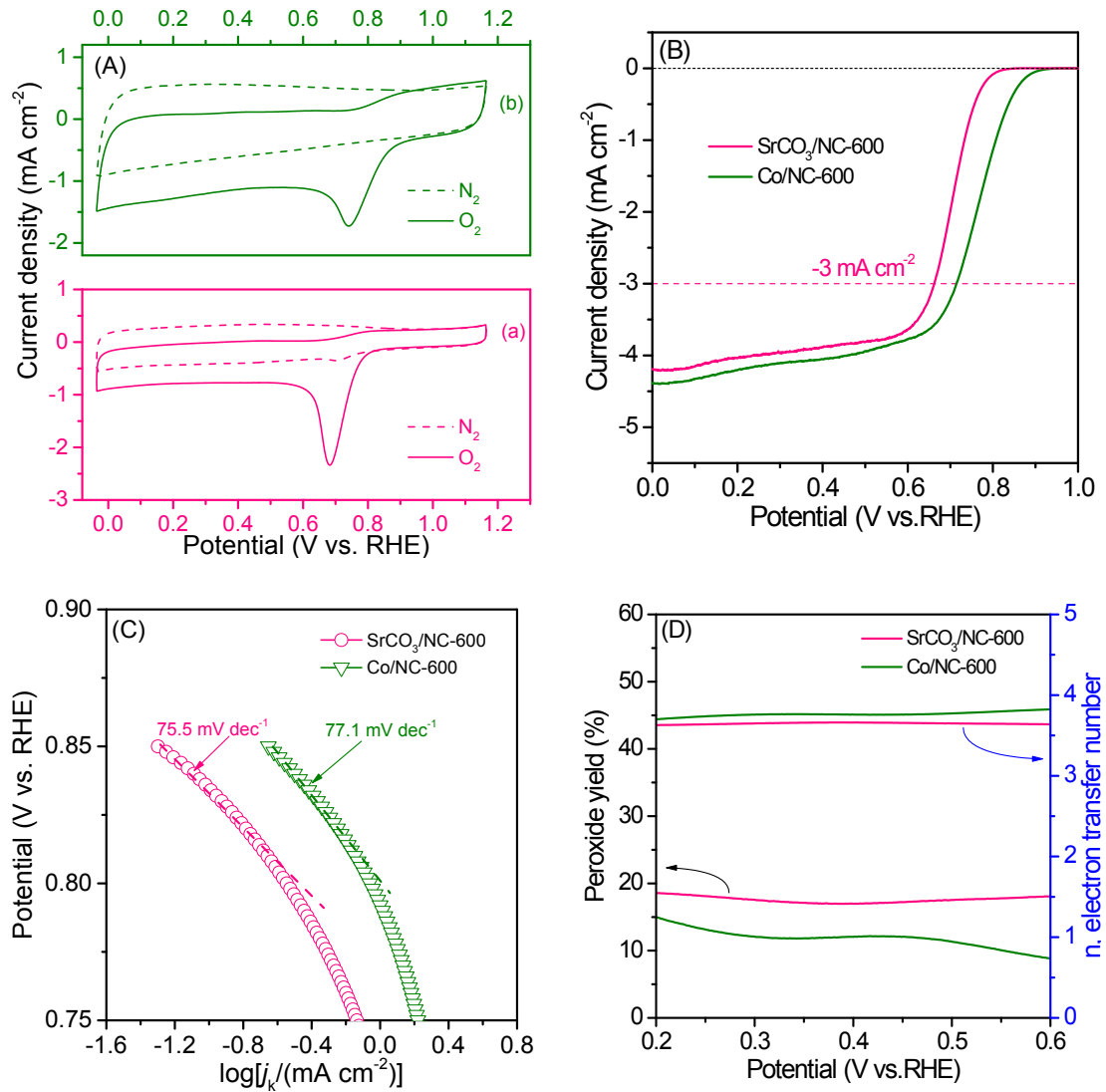


**Fig. S4.** (A) CV curves of  $\text{SrCO}_3/\text{NC-600}$  (a) and  $\text{Co}/\text{NC-600}$  (b) in  $\text{N}_2$  (dashed lines) and  $\text{O}_2$  (solid line) saturated 0.1 M KOH; (B) ORR LSV curves of  $\text{SrCO}_3/\text{NC-600}$  and  $\text{Co}/\text{NC-600}$ ; (C) Corresponding Mass-transport corrected Tafel plots at 1600 rpm; (D) Electron transferred number ( $n$ ) and peroxide yield of  $\text{SrCO}_3/\text{NC-600}$  and  $\text{Co}/\text{NC-600}$  at various potentials determined by RRDE.

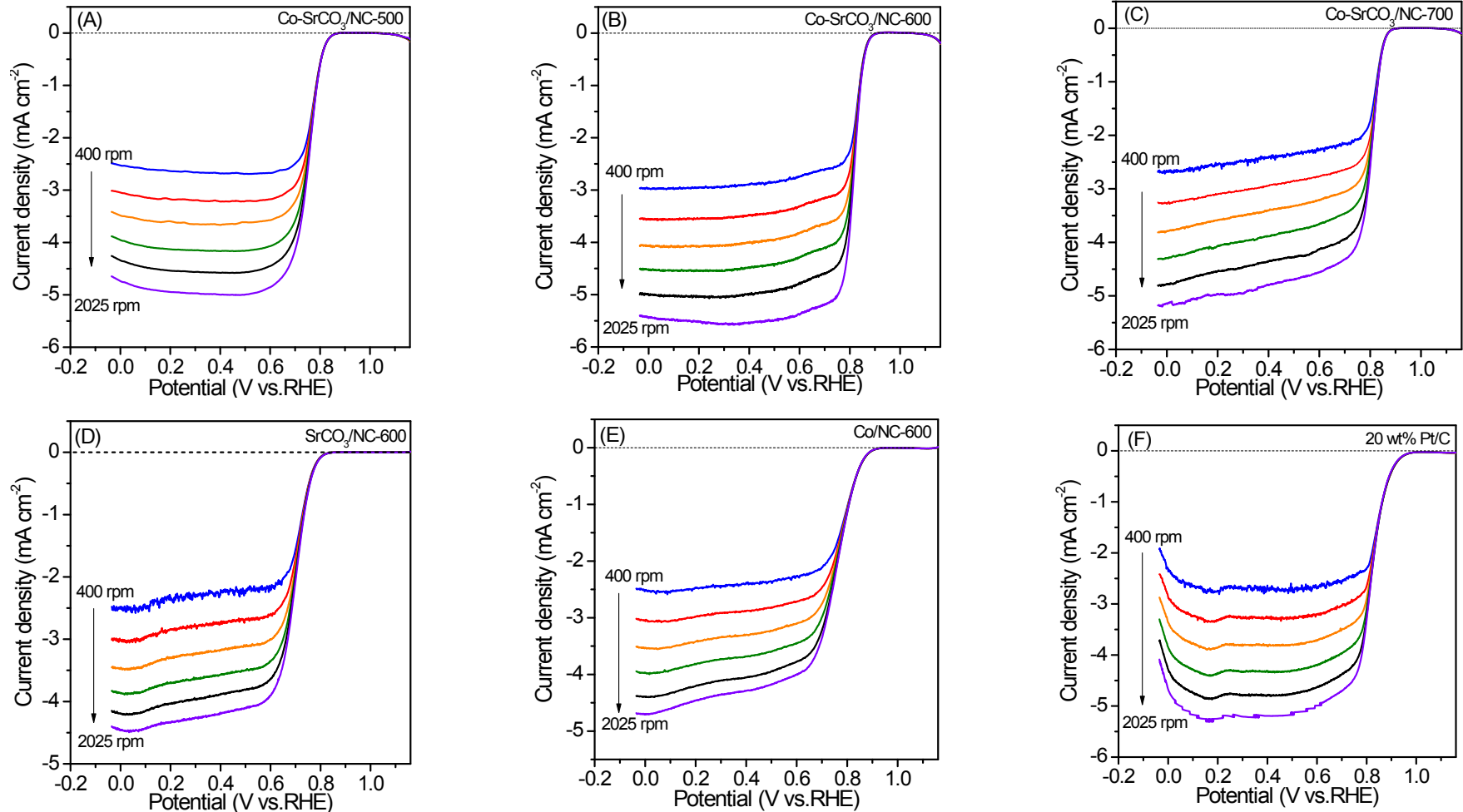


**Fig. S5.** RDE voltammograms for the prepared electrocatalysts, the reference samples and 20 wt% Pt/C under different rotational speeds (400,

625, 900, 1225, 1600 and 2015 rpm).

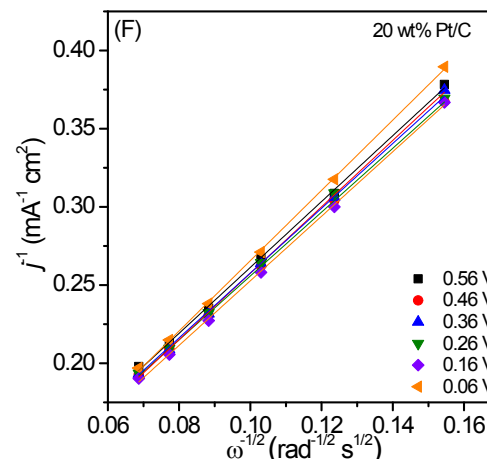
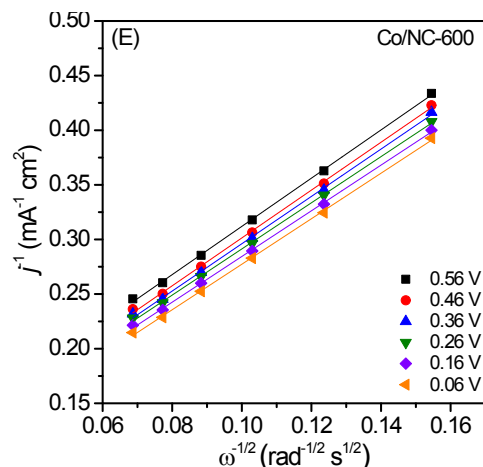
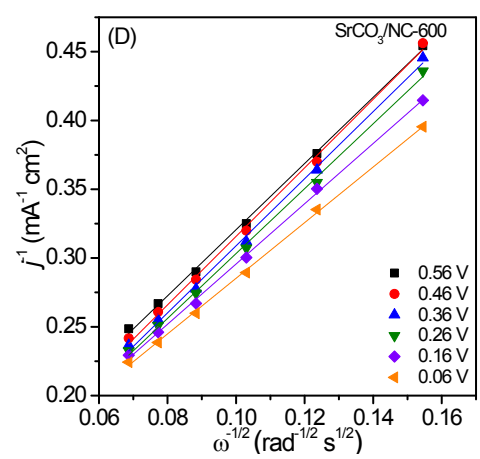
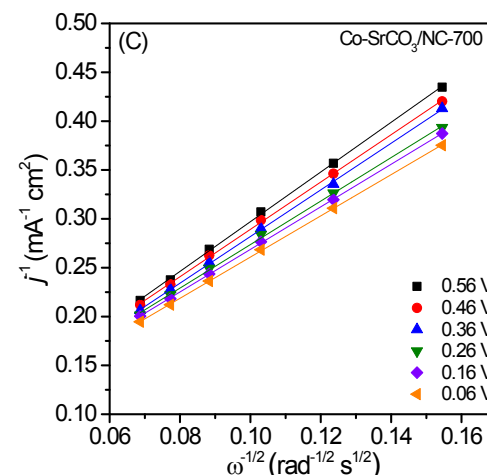
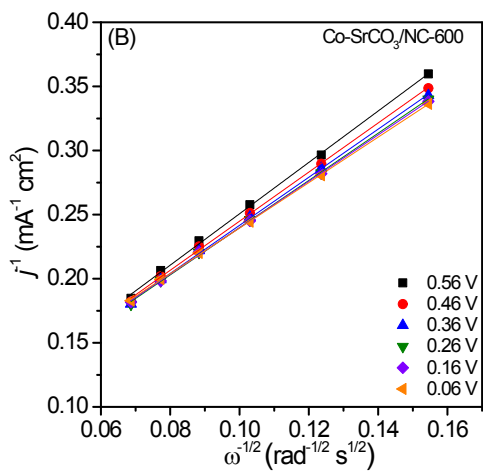
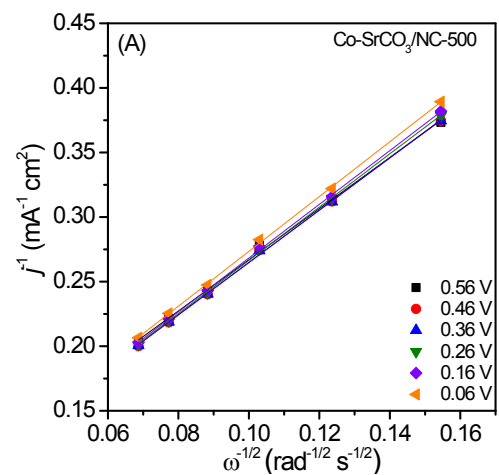


**Fig. S6** Koutecky-Levich (K-L) plots for the prepared electrocatalysts, the reference samples and 20 wt% Pt/C.

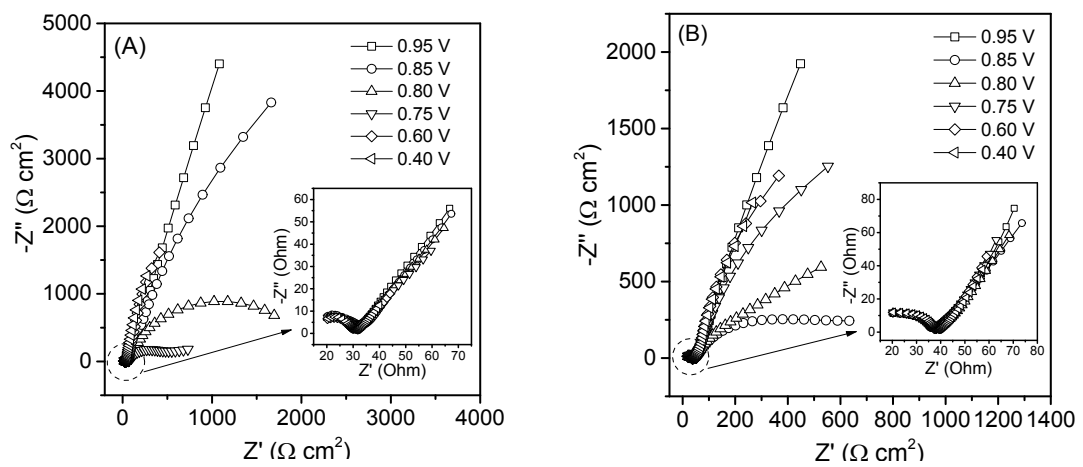


**Fig. S7** Nyquist plots of the electrode with SrCO<sub>3</sub>/NC-600 (A) and Co/NC-600 (B) at different ORR potentials.

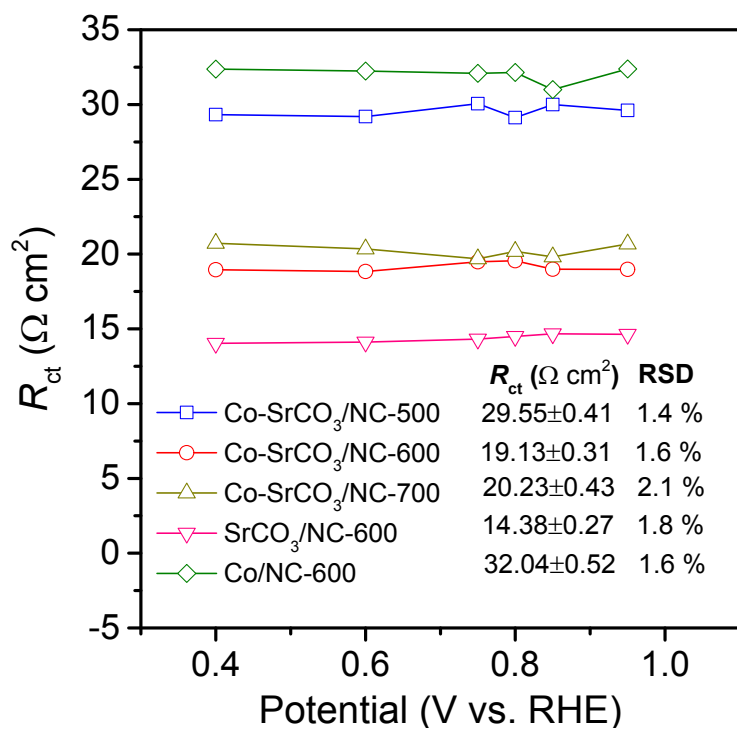


**Fig. S8** The potential-dependent  $R_{ct}$  values for Co-SrCO<sub>3</sub>/NC-500, 600 and 700, SrCO<sub>3</sub>/NC-600 and Co/NC-600, where RSD denotes the relative standard deviation.

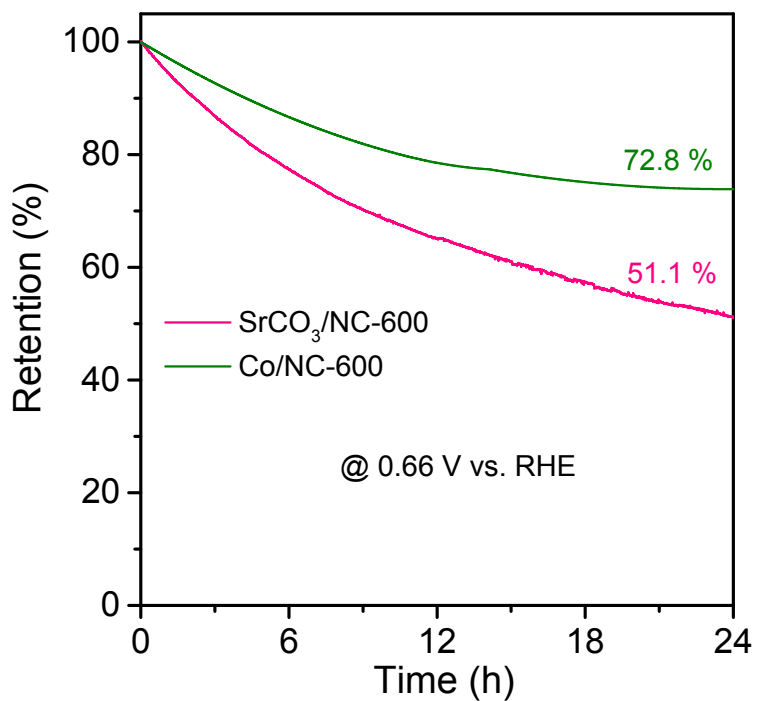


**Fig. S9.** The chronoamperometry (*i*-*t*) responses of  $\text{SrCO}_3/\text{NC}-600$  and  $\text{Co}/\text{NC}-600$  at 0.66 V (vs. RHE) in  $\text{O}_2$ -saturated 0.1 M KOH.

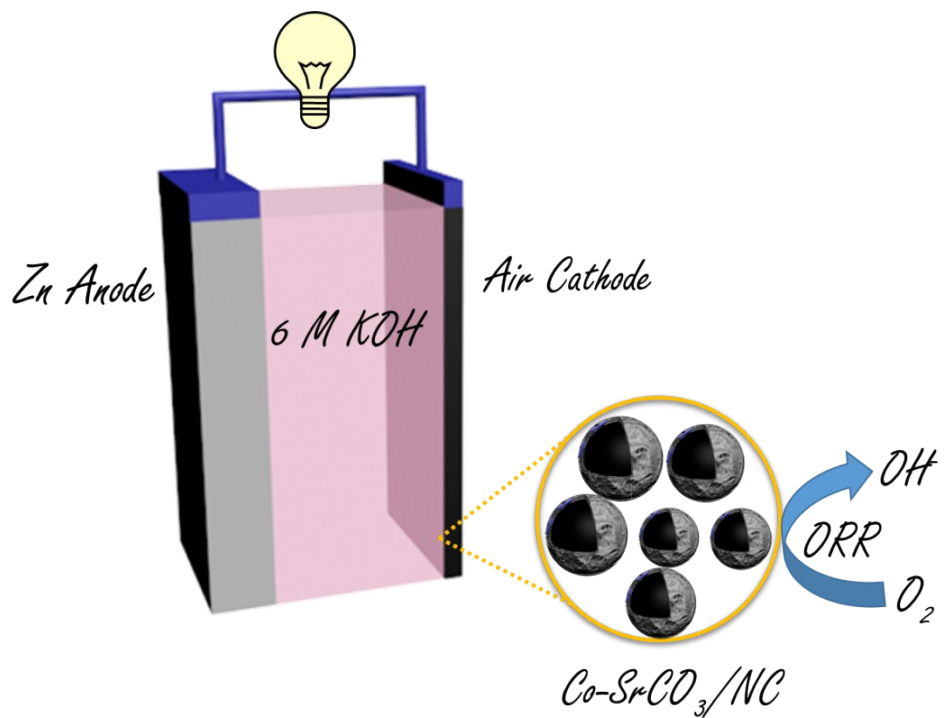


**Fig. S10.** Schematic illustration of a home-made Zn-air battery.

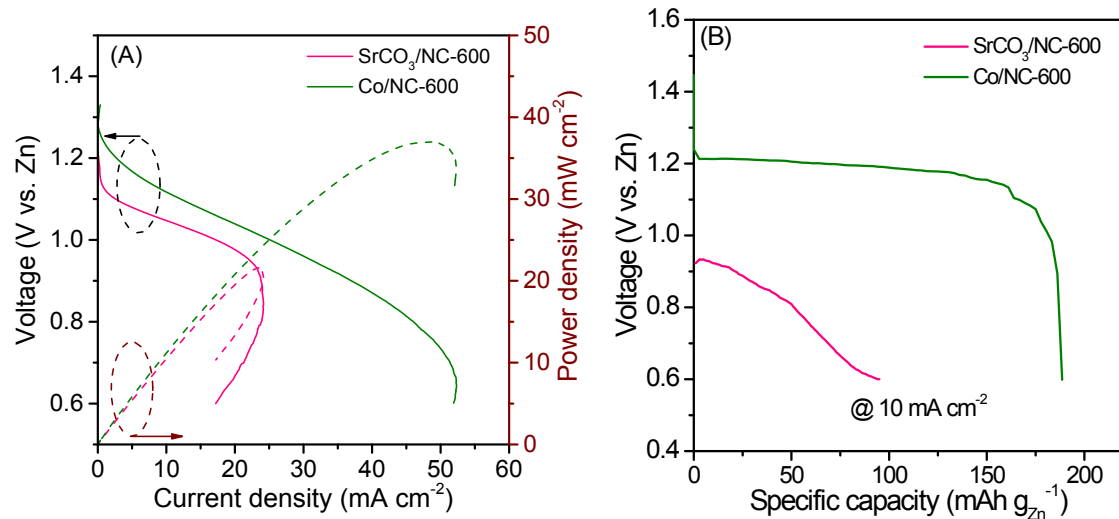


**Fig. S11.** (A) Polarization curves of Zn-air battery made with  $\text{SrCO}_3/\text{NC-600}$  and  $\text{Co}/\text{NC-600}$  air cathodes and the corresponding power density plots; (B) Long-time galvanostatic discharge curves of Zn-air battery with  $\text{SrCO}_3/\text{NC-600}$  and  $\text{Co}/\text{NC-600}$  air cathodes at  $10 \text{ mA cm}^{-2}$ .